



WATER OSCILLATIONS IN VERTICAL TUBES FOR APPLICATION TO DRAINAGE SYSTEMS

Schulz, Harry E.^{1,3}, Zhu, David Z.² and Ma, Yiyi²

¹ School of Engineering at São Carlos, University of São Paulo, Brazil

² Faculty of Engineering, University of Alberta, Canada

³ heschulz@sc.usp.br

Abstract: Vertical tubes are usual components of water distribution systems and of drainage systems (collecting tubes and manholes, for example). Drainage systems may be subjected to flooding events, which generate water columns with free surfaces in the vertical tubes. The water level corresponds, in these cases, to the hydraulic head where the vertical tube is located. Depending on the conditions of the flow in the system, pressure pulses may induce oscillations of the water level in the vertical tubes, eventually also generating phenomena like geysering. Oscillations may subject the buried structures to efforts not necessarily considered in the design phase. Eventual checking thus needs the periods of the oscillations. The amplitude of the oscillations may imply in spilling of water from the top section of the tube, or a momentary ejection above the outer ground level. The study of the conditions of possible spilling events is necessary to allow preventive measures. This study considers the dynamics of oscillating flows in vertical tubes. The governing equation for the flow is presented having the pressure imposed by the hydraulic head as the main impulsive factor of the movement. The resistive factors are taken into account through local and distributed losses. The equation is presented in normalized form, and predictions are compared with proper experimental data. Results obtained in adequate experimental devices, for different diameters of the vertical tube, were analyzed together. Conclusions about the different measured periods and the damping of fluctuations are presented.

Keywords: - Water oscillations in tubes, drainage systems, periods of oscillation, damping periodic flow, flooded manholes.

1 INTRODUCTION

The flooding of drainage systems in urban areas is becoming more common due to the accelerated increase of the cities, generating conditions not predicted in the design phase of these systems. This problem was already evidenced during the last two decades of the 20th century (Guo et al. 1990), but the frequency of flooding events is increasing since then (Lou et al. 2008, for example). Figures 1a and 1b sketch two conditions of possible flooding of urban drainage systems: the first showing only a flooded system of tubes, and the second showing a flood covering part of the surface of the urban area. The figure sketches vertical collectors, but also manholes may be considered. Implantation of new systems, extensions to existing systems, corrections of problematic sites, are procedures which design is based on existing or expected scenarios. If flooding is among these scenarios, the possibility of oscillations and geysering requires information of flow dynamics not only related to permanent and free surface cases. Computational tools allow the needed quantification, and calibration procedures are then followed.

Numerical codes for different transient situations in drainage systems may be found in the literature, some devoted to the transition from free to pressurized flows (Politano et al. 2005; Fuamba 2003, for

example), others to the fluctuations in surge tanks due to valve operations (Wang et al. 2015, for example). Codes calibration considers generally simple flow conditions, in order to quickly verify the accuracy of obtained answers of, for example, periods of oscillation, pressure, and velocities. Vertical tubes may be of interest for the oscillation calculations, and also for its damping through the use of oscillation suppressing devices, for protection of systems that may be subjected to some sudden blockage. In this case the tubes may be viewed as surge tanks, or, if capped, as air chambers, both viewed as a way of absorbing part of the energy of the flow oscillations.

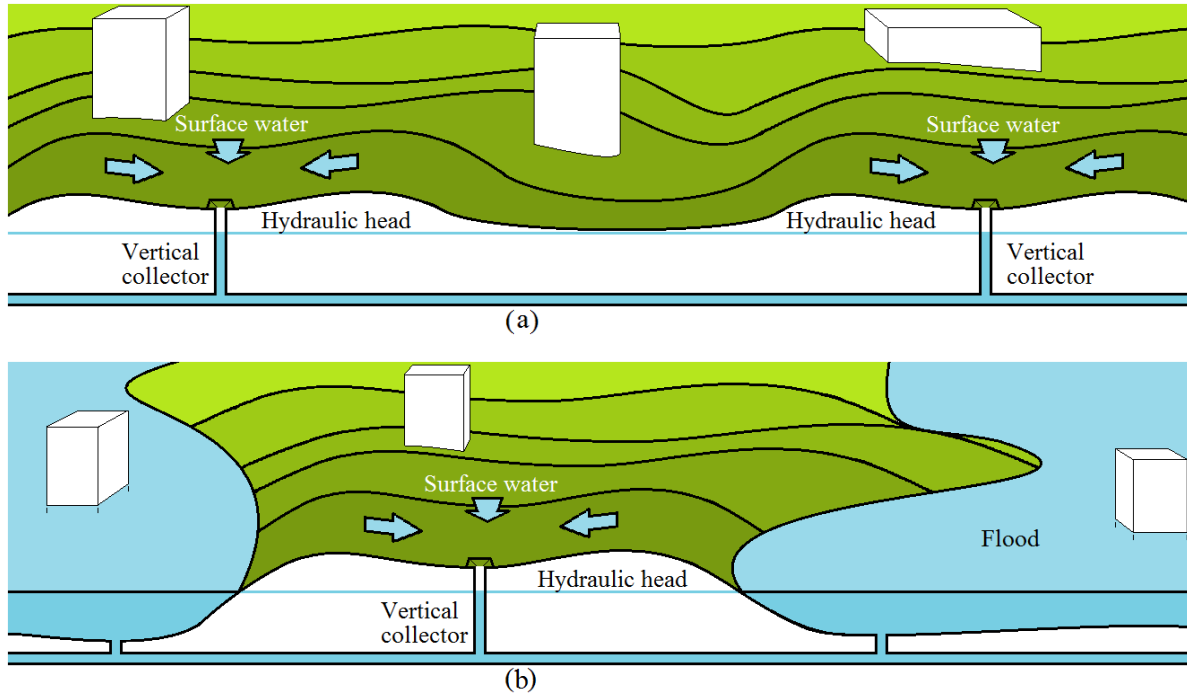


Figure 1: a) Flooded underground drainage system showing interconnected vertical collectors partially filled with water; b) Flood covering part of the urban surface area, and one vertical collector partially filled.

Complete drainage systems are simulated in the literature, but to provide a simple checking device, the vertical collector geometry was simplified in the present study as shown in Figure 2c.

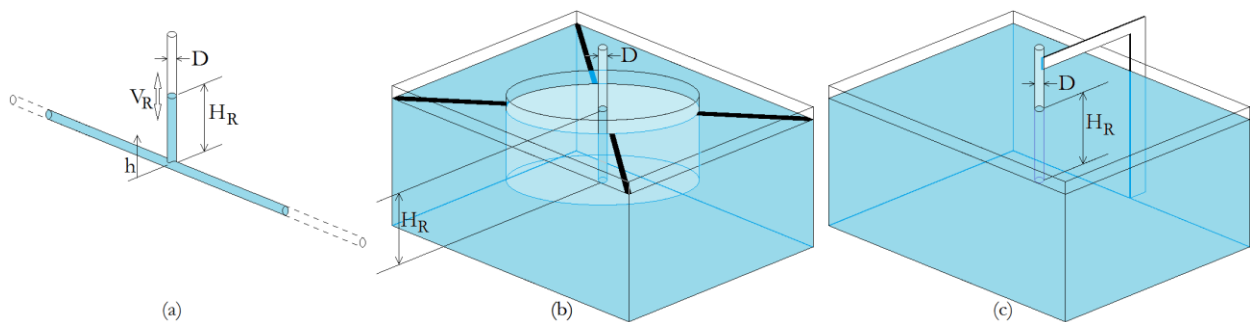


Figure 2 a) Real situation: vertical tube fixed to the horizontal system of tubes (shown in Figure 1); b) Possible laboratory setup: vertical column in a cylindrical empty reservoir which is fixed to the filled rectangular reservoir, c) Simplest setup of this study: only the vertical tube immersed in the rectangular reservoir. D is the diameter of the tube, H_R is the equilibrium position, V_R is the velocity, and h is the vertical axis that locates the water surface.

The oscillation in the vertical tube (collector, manhole, or tube for an oscillation suppressing device) was analyzed here considering two governing differential equations solved analytically and numerically. The

first is for the internal movement induced by an initial displacement from the equilibrium condition (H_R in Figure 2), considering concentrated and distributed losses in the vertical tube. The second is for the internal and external movements of the whole volume of water, for flows without losses. Comparisons with experimental data are presented. The experimental data were collected in devices properly built for this study. The aim of the study was to verify the applicability of the equations, in the sense of quantifying the periods of oscillation and the damping of the amplitudes in the geometry of vertical tubes.

2 MATHEMATICAL MODELS

The governing equation for the internal movement, induced by an imposed displacement from the equilibrium position (H_R), and considering local and distributed losses, is given by:

$$[1] \quad d^2y/dx^2 = (1/y - 1) + \theta_1(\theta_2 + \theta_3/y)(dy/dx)^2$$

In this equation, $y = h/H_R$, $\tau = t\sqrt{(h/H_R)}$, $\theta_1 = \pm 1$, $\theta_2 = fH_R/2D$, $\theta_3 = \sum_i(K_i/2)$, where t is the time, D is the diameter of the vertical tube, f is the friction factor (for distributed losses), and K_i are local loss coefficients ($i=1, 2, 3\dots$). Equation 1 was obtained applying the principles of conservation of mass, momentum, and energy to the flow of the vertical tube, having atmospheric pressure at the water surface. As can be seen, θ_2 and θ_3 may be dependent on the flow itself, because the friction factor and the local loss coefficient are functions of the internal Reynolds number. In the present study θ_2 and θ_3 were taken as constants, which allow obtaining theoretical solutions, and also allow quickly verifying the adequacy of the equation in comparison to experimental data. Because θ_2 and θ_3 are multiplied by the square of the velocity, the constancy of the coefficients gives a turbulent characteristic to the quantified losses. This equation was integrated for natural values of $2\theta_3$ (that is, $2\theta_3=1, 2, 3\dots$), furnishing theoretical solutions of the vertical velocity for different values of the summed local losses. For example, for $\theta_3=1$ and $\theta_2=1$ the solution is given by the set of Eqs. [2] and [3]:

$$[2] \quad V_{Up} = \sqrt{C_{Up}y^{-2}e^{-2y} - \left(1 - \frac{1}{y}\right)^2}$$

$$[3] \quad V_{Down} = \sqrt{e^{2y}y^2 \left[-\frac{e^{-2y}}{y^2} + 4\frac{e^{-2y}}{y} + 8\ln y + 8\sum_{i=1}^{\infty} (-2y)^i / (i \cdot i!) + C_{Down} \right]}$$

V is the nondimensional velocity $V=V_R/\sqrt{(gH_R)}$, where g is the acceleration of the gravity, and V_R is the dimensional (real) velocity, as shown in Figure 2a. C_{Up} and C_{Down} are integration constants, and must be determined for each cycle "up/down" of the oscillating column. θ_2 depends on the parameters of its definition, being $\theta_2 = 1.0$ used here as a convenient example. $2\theta_3 > 2$ produces more complicated equations. $2\theta_3 = 2$ and $\theta_2 = 1.0$ were used for upwards and downwards movements, but different values may be used for each direction of movement. Upwards and downwards flows are established by setting θ_1 as -1 and $+1$, respectively. The theoretical solutions, Eqs. [2] and [3] may be used for calibration procedures. When intending to adjust θ_2 and θ_3 to experimental data, the direct use of Eq. [1] is recommended, because it allows using non-integer values for the two coefficients. As can be seen, although the global movement is a sequence of up/down cycles, it is not expressed as a damped sinusoidal function, with the intrinsic period of 2π , but by two different equations for the "up" and "down" directions. This is evident by the use of $\theta_1 = +1.0$ or -1.0 in Eq. [1], and by the fact that each value of θ_1 leads to a different mathematical function for the movement. Although following different arguments and equations, similar conclusions are presented in the literature (Lorenceanu et al., 2002; Masoodi et al., 2013, González-Santander and Martín, 2014, for example).

As mentioned, Eqs. [1], [2] and [3] consider the water inside the vertical tube, which is surely the relevant aspect of the flow. However, the moving water system also involves water outside the tube. Figure 3a shows a sketch of the water moving internally and externally of the vertical tube (up and down arrows). The external area A_E shows the limitation of the horizontal spreading of the water. We firstly considered two "ideal" conditions:

1. the outer superficial area has the same value of the internal superficial area ($A_E = A_t$). In this case, the situation is similar to a “U tube”, which for a drainage system could be represented by the situation of Figure 1a. In this figure, if the right and left horizontal extensions of the drainage system are “closed” (momentously no flow), oscillations occur between the two vertical collectors, along a stretch of tube of constant area; and
2. the external area A_E tends to infinity. It corresponds to the sketch of Figure 1b, in which the oscillation occurs in the vertical collector, but it is not expected that the external level changes during the movement.

Figure 3b shows that the same experimental arrangement may be used to study much more complex situations, including long horizontal pipe systems by using coiled hoses. For the study of the vertical tubes only the arrangement of Figure 3a was used.

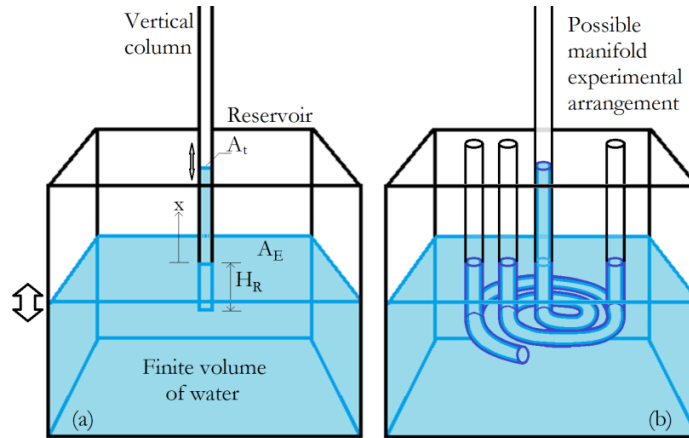


Figure 3: a) Whole moving volume of water. Origin of x at the equilibrium position, different of h of Figure 2. A_t is the transversal area of the tube, and A_E is the external superficial area; b) Example of possible complex arrangement allowed by this setup: manifold of vertical flows. The reference length may be more complex than only H_R .

The period of oscillation for the situation of Figure 3a is quantified here without considering shear losses (usual procedure in period evaluations). The governing Eq. [4] is used, and may be obtained by applying the energy conservation principle, or the balance of forces:

$$[4] \quad gx + \frac{\beta}{2} (dx/dt)^2 + (H_R + \beta x) d^2x/dt^2 = 0 \quad , \quad \text{where} \quad \beta = 1 - (A_t/A_E).$$

A_t is the transversal area of the tube, and A_E is the external superficial area. Equation [1] was integrated once to furnish the velocity of the flow in the tube using $dx/dt = 0$ at $x = x_0$, being x_0 the initial height of the water in the tube, leading to Eq. [5], presented here using nondimensional groups:

$$[5] \quad d\left(\frac{x}{x_0}\right) / d\sqrt{\frac{g}{H_R}} t = \pm \sqrt{\left[1 - \left(\frac{x}{x_0}\right)^2\right] / \left[1 + \sigma\left(\frac{x}{x_0}\right)\right]} \quad , \quad \text{where} \quad \sigma = \frac{\beta x_0}{H_R}.$$

If $\beta = 0$, the transversal area of the flow is constant, corresponding to a “U” tube, with the governing equation and its solution for $x = x_0$ at $t = 0$ presented as Eq. [6]:

$$[6] \quad d\left(\frac{x}{x_0}\right) / d\sqrt{\frac{g}{H_R}} t = \pm \sqrt{1 - (x/x_0)^2} \quad , \quad \text{thus} \quad \frac{x}{x_0} = \cos\left(\sqrt{\frac{g}{H_R}} t\right).$$

The period is $T = 2\pi\sqrt{(H_R/g)}$. In U tubes the total length (L) of the water volume is used, that is, $H_R = L/2$. For $\beta \rightarrow 1$, which implies $A_E \rightarrow \infty$, Eq. [5] may demand more efforts to be integrated. Considering, for

simplicity, $H_R = x_0$, the governing equation and its solution are reduced, for $0 \leq x \leq x_0$, to the forms shown in Eqs. [7]:

$$[7] \quad d\left(\frac{x}{x_0}\right) / d\sqrt{\frac{g}{H_R}} t = -\sqrt{1 - (x/x_0)} \quad , \quad \text{thus} \quad \frac{x}{x_0} = 1 - \frac{1}{2} \left(\sqrt{\frac{g}{H_R}} t\right)^2 .$$

The time consumed moving along $0 \leq x \leq x_0$ is $t = 2\sqrt{(H_R/g)}$. The period for the surface of the water to return to the initial position is $T = 4t$, or $T = 8\sqrt{(H_R/g)}$ (remembering that $H_R = x_0$ in this derivation). As comparison tool, we may express $8 \approx 2.54\pi$. $\beta = 0$ leads to a sinusoidal function and to factor 2π for the fundamental period, while $\beta = 1$ conduces to a succession of parabolas and to the factor 2.54π for the period. The two functions are plotted in Figure 4a. Thus, for $H_R = x_0$ the periods of oscillation predicted by Eq. [5] are in the range $2\pi\sqrt{(H_R/g)} \leq T \leq 2.54\pi\sqrt{(H_R/g)}$, or, using the exact value, $2\pi\sqrt{(H_R/g)} \leq T \leq 8\sqrt{(H_R/g)}$. The possibility of different results considering or not the inertia of the water tank is mentioned in numerical studies of the literature, although not related to conceptual derivations as done here (Wang et al. 2015).

Equation [5] allows more detailed discussion. Considering the factor $\sigma = \beta x_0/H_R$, it tends to zero when $H_R \rightarrow \infty$, for any β and x_0 . In other words, for long tubes (like the horizontal tubes in drainage systems), the period tends to $2\pi\sqrt{(H_R/g)}$ (in drainage systems $H_R = L/2$, being L the immersed length of the tubes, not only the hydraulic head). The condition $\beta = 1$ ($A_E \rightarrow \infty$) needs analyses of the effect of $\sigma = x_0/H_R$ on the period of vertical tubes. Figure 4b shows the evolution of x/x_0 for the first quarter of a period ($0 \leq x \leq x_0$) using different values of σ . Equation [6] implies $\sigma = 0$ and the period $2\pi\sqrt{(H_R/g)}$, so that any $\sigma > 0$ leads to larger periods. This occurs more evidently for the first periods. Along time, energy losses damp the amplitudes of the oscillations, producing smaller σ for each new period, probably inducing also a trend to $T = 2\pi\sqrt{(H_R/g)}$ for the larger times. Finally, the ideal and real conditions of flows for $\beta = 1$ are sketched in Figure 5, showing that in real cases the whole external volume of fluid does not dislocate with a homogeneous vertical velocity. A smaller amount of water dislocates vertically (closer to the tube), with a correspondent smaller mean A_E . As a conclusion, periods with value $T = 2\pi\sqrt{(H_R/g)}$ and larger are expected for vertical tubes, although smaller than the ideal period $T = 2.54\pi\sqrt{(H_R/g)}$.

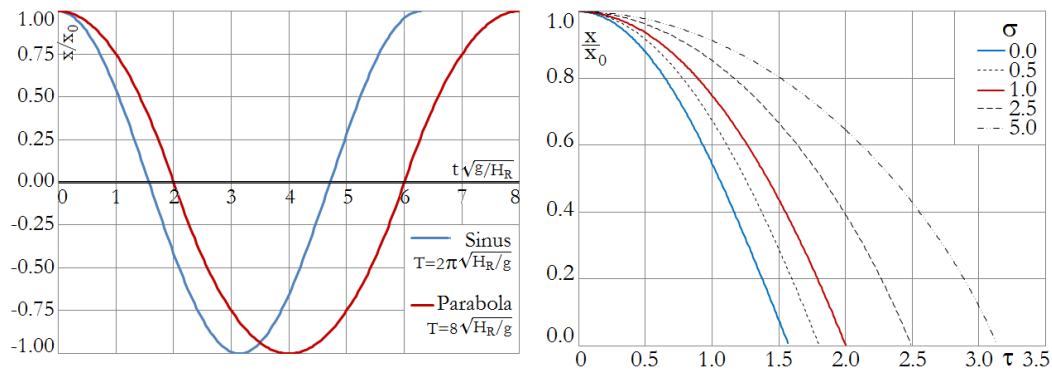


Figure 4: a) Shear free evolution of the water surface for $\beta = 0$ and $\beta = 1$ for vertical tubes; b) Shear free evolution for the first quarter of a period given by Eq. [5] for different σ . ($\tau = t\sqrt{(g/H_R)}$).

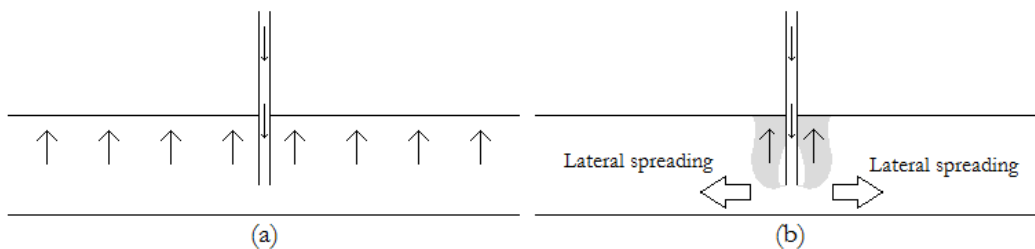


Figure 5: a) Ideal situation $\beta = 1$: fluid moves vertically with homogeneous velocity extending horizontally to infinity; b) Real situation: the fluid has a main vertical movement that does not extends to infinity.

3 EXPERIMENTAL DEVICES

Experiments were conducted in the Hydraulics Laboratory of the University of Alberta following the sketch of Figure 3. Two small scale devices were built for experiments conducted with tubes having diameter of 0.62 cm and 2.54 cm. A third larger scale setup was built for a vertical tube with diameter of 10.16 cm. The larger setup is shown in Figure 6a. A cast acrylic tube was used, with internal diameter of 4" (10.16 cm), and external diameter of 4½" (11.43 cm). The superficial area of the water tank was 1.769 m², having a square shape with sides of 1.33 m. The total height of the tank was about 91 cm, but experiments were also run for a depth of about 75 cm. The length of the acrylic tube was about 1.84 m.

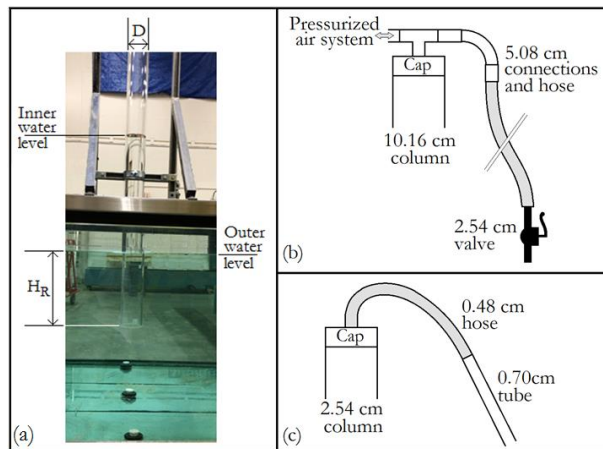


Figure 6: a) Experimental setup for column with $D = 10.16$ cm. b) Details of the control of the air flow for column with $D = 10.16$ cm. c) Details of the control of the air flow for column with $D = 2.54$ cm. The numbers in the figure are diameter values.

For the experiments with $D = 10.16$ cm, the upper section of the vertical column was covered with a cap fixed to a hose with a diameter of 5.08 cm (2"), using a "T" and a "curve" connections with a total length of 60 cm. The hose had a length of 4.11 m. A manual "open/close" valve was installed at the open end of the hose using a 10 cm long connection. Valve and connection had diameter of 2.54 cm (1"). The second opening of the "T" connection at the tube cap was used to inject air or to produce vacuum in the vertical column, for the adjustment of the inner water level. A sketch is shown in Figure 6b. Experiments were conducted in two ways: 1) by removing the cap and opening completely the end on the vertical tube, and 2) by opening the valve at the end of the hose. Thus free oscillations and damped oscillations were produced, respectively.

For the experiments with $D = 2.54$ cm, a plastic tube with length of 45.5 cm was used. Also for this diameter, the upper section of the vertical column was covered with a cap fixed to a hose. The hose was 30 cm long and had a diameter of 0.48 cm, being connected to a straight tube 21.5 cm long and with a diameter of 0.70 cm. The water in the vertical tube was adjusted by blowing in the 0.70 cm tube. A sketch is shown in Figure 6c. Also here experiments were conducted in two ways: 1) by removing the cap and opening completely the end on the vertical tube, and 2) by opening the end of the 0.70 cm tube. Once more, free oscillations and damped oscillations were produced, respectively.

For the experiments with $D = 0.62$ cm, a plastic tube 31.2 cm long was used. Considering the small diameter, only free oscillations were conducted in this tube. In this case capillary effects were present, thus involving forces not considered in the original formulation that also helped the damping of the oscillations.

The data were collected by filming the experiments with digital cameras, using speeds of 200, 120, 60, 40, and 30 fps. It was observed that higher speeds are more adequate (200, 120, and 60 fps) for the present experiments.

4 RESULTS

4.1 Periods of Oscillation

The theoretical calculations presented here in Eqs. [4] to [7] showed two possible “ideal” periods for shear free oscillations and $x_0 = H_R$: 2π and 8 (or 2π and $\sim 2.54\pi$), with a difference of 27%. As already mentioned, also numerical results of the literature show that different periods may be calculated for the same physical situation (Wang et al. 2015), depending on the adopted assumptions. Because such different results, the knowledge of the behavior of real data is necessary. The experiments were conducted using the vertical tubes with $D = 10.16$ cm, 2.54 cm, and 0.62 cm. Table 1 shows the experimental conditions and the measured periods, which were extracted from the post-processing of the obtained films. The post-processing involved frame by frame analyses for the location of the water surface, and the registering of the results. Corrections of refraction effects were performed.

Table 1: Experimental conditions and measured periods for vertical tubes

Free/Damped	Diameter (cm)	H_R (cm)	Measured Period (s)
Damped	10.16	22.5	1.008
Free	10.16	19.3	0.972
Damped	10.16	19.9	0.976
Free	10.16	19.0	0.970
Damped	10.16	33.6	1.287
Damped	10.16	33.6	1.279
Damped	10.16	41.2	1.400
Free	10.16	41.0	1.418
Damped	2.54	18.2	0.908
Free	2.54	18.2	0.878
Free	0.62	7.5	0.535
Free	0.62	5.8	0.500

The dots of Figure 7 show the measured periods of oscillation plotted against the measured $\sqrt{(H_R/g)}$. The lower and upper lines are the predictions of Eqs. [6] and [7], respectively. For smaller $\sqrt{(H_R/g)}$ the measured periods are closer to the line $T = 2\pi\sqrt{(H_R/g)}$, but they depart from this line for larger $\sqrt{(H_R/g)}$. The best fit of the data is $T = 2.17\pi\sqrt{(H_R/g)}$, with $R^2 = 0.99$, located between the two theoretical predictions.

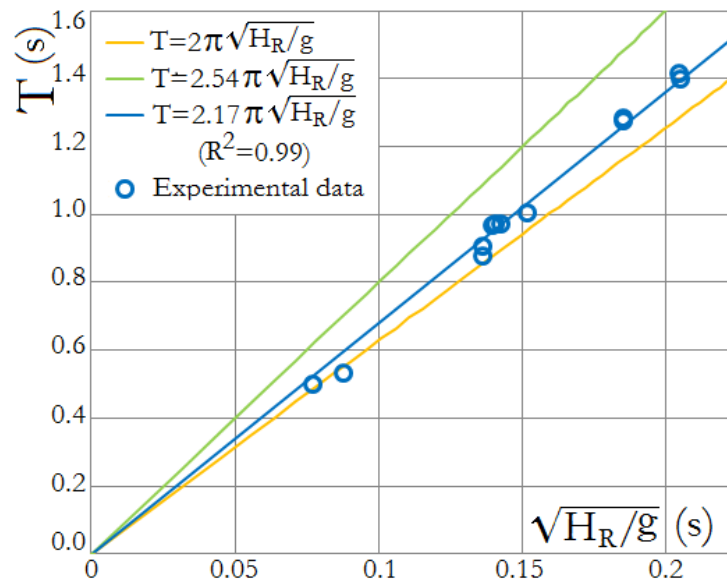


Figure 7: Theoretical and experimental results for the periods of oscillation in vertical tubes.

4.2 Damping of Oscillations

The calculation of oscillations in flooded scenarios allows verifying the distribution of additional efforts due to the water flow. But they may also suggest the use of devices that suppress the oscillations, intending to avoid induced damages. This study generated data for damped situations, for which a control of the air flow was applied. The top air pocket with the hose described in Figure 6 is the oscillation suppressing device used in the present study. In order to test Eq. [1], free oscillations experiments were firstly conducted by removing the cap of the vertical column and letting the air flow without restrictions. Experimental results and numerical calculations using Eq. [1] are shown in Figure 8 for $D = 2.54$ cm. Figure 8a shows the nondimensional water level plotted against the nondimensional time, and Figure 8b shows the nondimensional vertical velocity plotted against the nondimensional level.

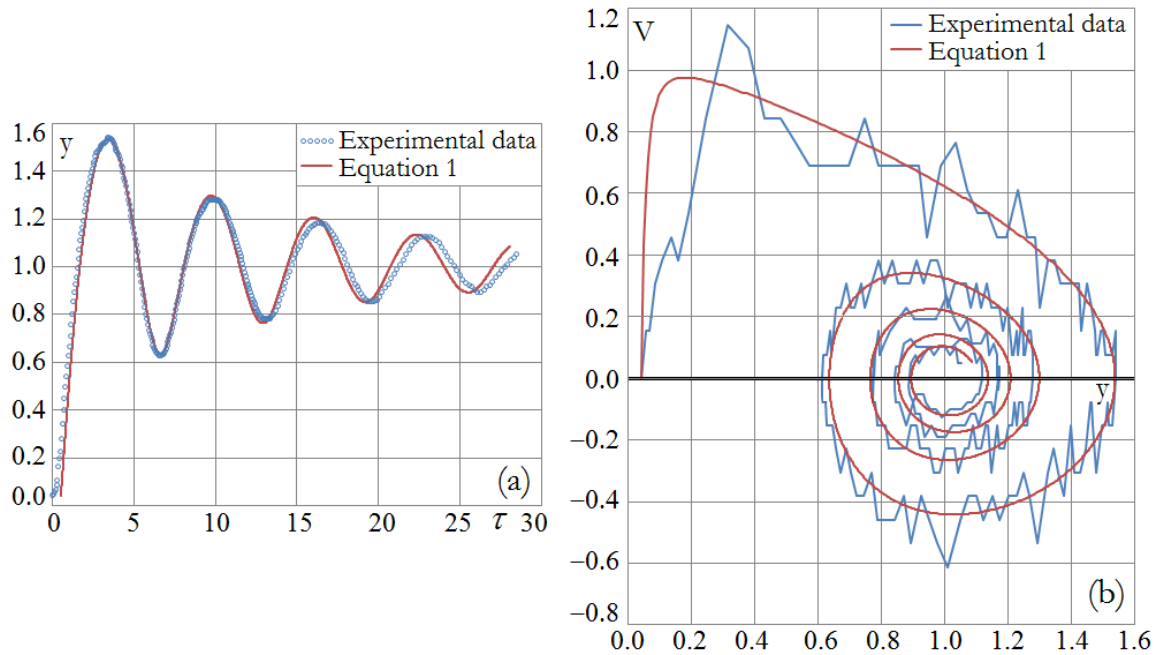


Figure 8: a) Measured and calculated water levels, $D = 2.54$ cm. Theoretical results with a shift $t_0 = 0.4$ (column uncapping lead to an experimental lag time); b) Measured and calculated velocities, $D = 2.54$ cm.

The calculations were performed using constant values of the coefficients θ_2 and θ_3 for each up/down movement, as follows: First and second up: $\theta_2 = 0.1$, and $\theta_3 = 0.85$; first and second down: $\theta_2 = 0.1$, and $\theta_3 = 0.01$, subsequent up and downs: $\theta_2 = 0.1$, and $\theta_3 = 0.85$. The adjustment to the observed movement is good, for both the water level and the velocity. The observed difference for higher times may be caused by the use of constant θ_2 and θ_3 for each up/down movement. These coefficients are functions of the movement itself (expressed through the Reynolds number, for example).

The damped oscillations shown in Figure 9 were produced by opening the valve and the straight tube in the setups for $D = 10.16$ cm and $D = 2.54$ cm, respectively. The air cap was maintained, so that pressurized air chambers were formed above the water level, together with high loss regions along the hoses. Figure 9a shows the evolution of the nondimensional water level of damped experiments for $D = 10.16$ cm and $D = 2.54$ cm, while Figure 9b shows the evolution of the nondimensional velocity for $D = 10.16$ cm. Numerical predictions would need Eq. [1] for the water flow and an additional equation for the air flow, not discussed in the present study.

A first evaluation of the suppression of oscillations was made based on the initial positive or negative pulse P_0 , given as $P_0 = |y_0 - 1|$ (modulus was used, that is, positive values). It corresponds to a sudden lack or excess of pressure (in relation to the equilibrium level) applied at the basis of the vertical tube used as

oscillation suppressing device. The capacity to reduce initial pulses was analyzed through the subsequent $P_1 = y_1 - 1$ and $P_2 = y_2 - 1$ values, using the first maximum and minimum of the experimental y function. Table 2 shows values obtained for free and damped experiments with $D = 10.16$ cm and $D = 2.54$ cm.

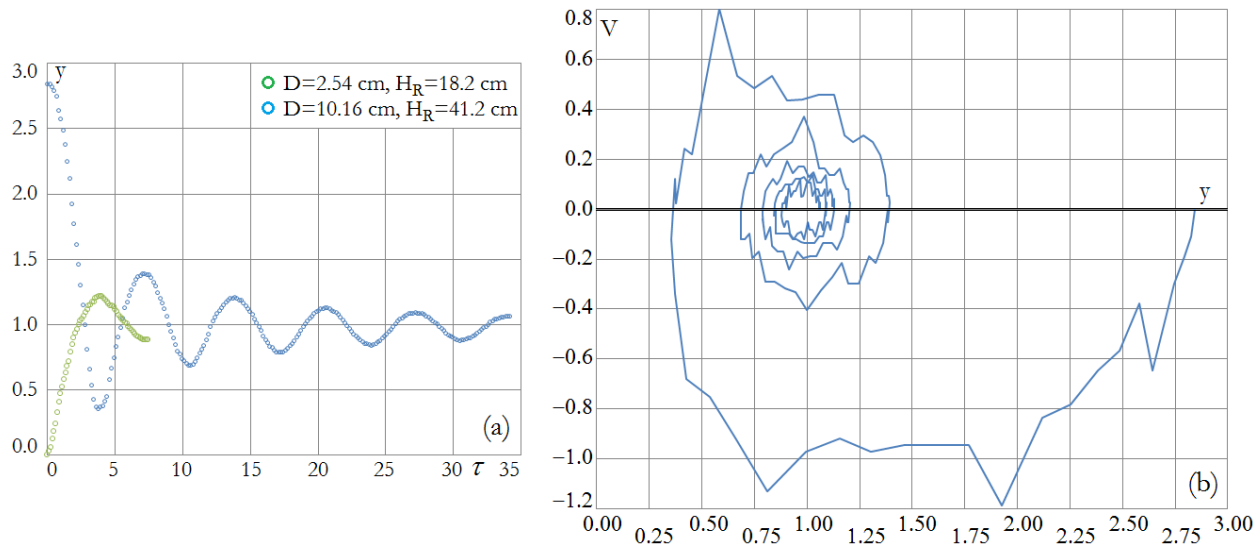


Figure 9: a) Experimental damped water levels; b) Experimental damped velocities for $D = 10.16$ cm.

The last column of Table 2 shows that the 10.16 cm vertical tube reduces to about 34.9% the initial pulse for one oscillation period (P_2) when working like an open surge tank (free oscillations). When using the air chamber and the hose, the reduction attains about 21.3% of the initial pulse. The same sequence for the 2.54 cm vertical column shows the results of 37.4% for free oscillations, and 11.6% for the air chamber with hose. The half period analysis (P_1) is possible for the 2.54 cm tube, showing the results of 54.2% for free oscillations, and 21.5% for air chamber with hose. The half period analysis is not possible for the 10.16 cm tube because the experimental procedures did not furnish the internal water levels when below the external water level. The results show that the experimental setup allows the study of suppression of oscillations, through the comparative analysis of free and damped oscillations, the last understood as being damped through an installed device.

Table 2: Reduction of oscillations for free and damped experiments (modulus of P_i were used)

Free/Damped	Diameter (cm)	H_R (cm)	P_0	P_1	P_2	P_1/P_0	P_2/P_0
Free	10.16	41.0	1.78	(*)	0.622	(*)	34.9%
Damped	10.16	41.2	1.84	0.648	0.391	35.2%	21.3%
Free	2.54	18.2	1.00	0.542	0.374	54.2%	37.4%
Damped	2.54	18.2	1.00	0.215	0.116	21.5%	11.6%

* P_1 not collected: internal water level not measured below the external water level.

5 CONCLUSIONS

Governing equations for the study of oscillating flows in vertical tubes were presented. A first equation considered the internal flow with energy losses, and a second equation considered the whole volume of water without energy losses.

Experimental setups were built in order to check with real data the theoretical predictions of the proposed equations. It was shown that the periods of oscillation in vertical tubes are preferentially larger than the solution $T = 2\pi\sqrt{(H_R/g)}$. The best fit equation for the present data was $T = 2.17\pi\sqrt{(H_R/g)}$, with a correlation coefficient $R^2 = 0.99$.

Numerical predictions for the evolution of the water level in the vertical tube are in good agreement with the measured results, a fact more evident for the first periods of oscillation. Differences observed for larger times are understood as a consequence of the use of constant friction factors and local loss coefficients in the numerical model (which in fact are dependent on the flow itself).

The use of the experimental devices to quantify observed damping in oscillation suppressing devices was tested. The initial condition was adjusted, and the subsequent maxima and minima were compared for free and damped oscillations, allowing the aimed direct comparison.

The obtained results show the adequacy of the methodology being followed in this research line.

Acknowledgements

The first author thanks the support of CAPES, which, through process BEX 5723/15-9, allowed the collaboration study with the University of Alberta. The authors thank Mr. Perry Fedun for the careful building of the larger experimental setup

References

- Fuamba, M. 2003. Contribution on Transient Flow Modelling in Storm Sewers. *Journal of Hydraulic Research*, **40**(6): 685-693.
- González-Santander, J.L. and Martín, G. 2015. New Analytical Approximations for the Liquid Rise in a Capillary Tube. *Fluid Dynamics Research*, **47**, 28p.
- Guo, Q. and Song, C.C.S. 1990. Surging in Urban Storm Drainage Systems. *Journal of Hydraulic Engineering*, **116**(12): 1523-1537.
- Lorenceanu, É.; Quéré, D.; Jean-Yves, O. and Clanet, C. 2002. Gravitational Oscillations of a Liquid Column in a Pipe. *Physics of Fluids*, **14**(6), 1985-1992.
- Lou, S.; Zhong, G.H.; Zhu, Y.D. and Liu, S.G. 2008. Investigation of Underground Traffic Facilities for Flood Control in Shanghai. *5th China-Japan Joint Seminar for the Graduate Students in Civil Engineering*, Tongji University, Shanghai, China, Proceedings, 136-141.
- Masoodi, R.; Languri, E.; and Ostadhossein, A. 2013. Dynamics of Liquid Rise in a Vertical Capillary Tube. *Journal of Colloid and Interface Science*, **389**, 268-272.
- Politano, M.; Odgaard, J. and Klecan, W. 2005. Numerical Simulation of Hydraulic Transients in Drainage Systems. *Mecánica Computacional*, **XXIV**: 297-310.
- Wang, C.; Yang, J. and Nillson, H. 2015. Simulation of Water Level Fluctuations in a Hydraulic System Using a Coupled gas-Liquid Model. *Water*, **7**: 4446-4476.